Conformational changes in the metal-binding sites of cardiac troponin C induced by calcium binding

ARTICLE *in* BIOCHEMISTRY · MARCH 1992

Impact Factor: 3.02 · DOI: 10.1021/bi00121a003 · Source: PubMed

4 AUTHORS, INCLUDING:

Rui M M Brito
University of Coimbra
61 PUBLICATIONS **972** CITATIONS
SEE PROFILE

John A Putkey
University of Texas Health Science Center at …
78 PUBLICATIONS **2,067** CITATIONS
SEE PROFILE

Paul R Rosevear
University of Cincinnati
80 PUBLICATIONS **2,058** CITATIONS
SEE PROFILE

Conformational Changes in the Metal-Binding Sites of Cardiac Troponin C Induced by Calcium Binding†

George A. Krudy, Rui M. M. Brito, John A. Putkey, and Paul R. Rosevear*
Department of Biochemistry and Molecular Biology, University of Texas Medical School at Houston, Houston, Texas 77225
Received August 20, 1991; Revised Manuscript Received November 4, 1991

ABSTRACT: Isotope labeling of recombinant normal cardiac troponin C (cTnC3) with ^{15}N-enriched amino acids and multidimensional NMR were used to assign the downfield-shifted amide protons of Gly residues at position 6 in Ca^{2+}-binding loops II, III, and IV, as well as tightly hydrogen-bonded amides within the short antiparallel β-sheets between pairs of Ca^{2+}-binding loops. The amide protons of Gly70, Gly110, and Gly146 were found to be shifted significantly downfield from the remaining amide proton resonances in Ca^{2+}-saturated cTnC3. No downfield-shifted Gly resonance was observed from the naturally inactive site I. Comparison of downfield-shifted amide protons in the Ca^{2+}-saturated forms of cTnC3 and CBM-IIA, a mutant having Asp65 replaced by Ala, demonstrated that Gly70 is hydrogen bonded to the carboxylate side chain of Asp65. Thus, the hydrogen bond between Gly and Asp in positions 6 and 1, respectively, of the Ca^{2+}-binding loop appears crucial for maintaining the integrity of the helix–loop–helix Ca^{2+}-binding sites. In the apo- form of cTnC3, only Gly70 was found to be shifted significantly downfield with respect to the remaining amide proton resonances. Thus, even in the absence of Ca^{2+} at binding site II, the amide proton of Gly70 is strongly hydrogen bonded to the side-chain carboxylate of Asp65. The amide protons of Ile112 and Ile148 in the C-terminal domain and Ile36 in the N-terminal domain β-sheets exhibit chemical shifts consistent with hydrogen-bond formation between the pair of Ca^{2+}-binding loops in each domain of Ca^{2+}-saturated cTnC3. In the absence of Ca^{2+}, no strong hydrogen bonds were detected between the β-strands in the N-terminal domain of cTnC3. Thus, Ca^{2+} binding at site II results in a tightening of the Ca^{2+}-binding loop and formation of one strong hydrogen bond between β-strands in the N-terminal domain. These changes may initiate movement of helices in the N-terminal domain responsible for the interaction of TnC with troponin I.

Troponin C (TnC)[1] is the Ca^{2+} regulatory protein of the troponin complex responsible for initiating contraction in striated muscle. The binding of Ca^{2+} to TnC induces a conformational change which is transmitted to the other components of the troponin complex and results in the release of inhibition of the myosin ATPase activity which leads to muscle contraction (Zot & Potter, 1987; Brenner, 1989). There are two isoforms of TnC: one isoform is found in fast skeletal muscle (sTnC) and the other is found in cardiac and slow skeletal muscle (cTnC). Although both isoforms have four potential Ca^{2+}-binding sites, sites I–IV, site I in cTnC is inactive (Van Eerd & Takahashi, 1975, 1976; Collins et al., 1977). Recently, the cDNA for chicken cTnC was incorporated into a bacterial expression system, and the bacterially produced protein (cTnC3) was found to be functionally identical to tissue-derived protein (Putkey et al., 1989; Sweeney et al., 1990). A functionally inactive mutant (CBM-IIA), which is unable to bind calcium at site II as a result of the conversion of Asp65 to Ala, directly demonstrated that Ca^{2+} binding to site II is responsible for initiating muscle contraction (Putkey et al., 1989). NMR studies have shown that the inability of CBM-IIA to trigger muscle contraction is due to inactivation of site II and not the effect of mutation on the conformation or stability of the protein (Brito et al., 1991).

The crystal structures of turkey and chicken sTnC showed this isoform to consist of two globular domains separated by a 31-residue α-helix (Herzberg & James, 1985, 1988; Herzberg et al., 1986; Sundaralingam et al., 1985; Satyshur et al., 1988). Both the N- and C-terminal domains contain a pair of helix–loop–helix Ca^{2+}-binding motifs. Calcium-binding sites III and IV, located in the C-terminal domain, have high affinity for Ca^{2+} and also bind Mg^{2+} but with lower affinity (Van Eerd et al., 1975; Potter & Gergely, 1977; Collins et al., 1977). Calcium-binding site II in cTnC and sites I and II in sTnC bind Ca^{2+} specifically, but with lower affinity than sites III and IV (Potter & Gergely, 1977; Holroyde et al., 1980). Calcium-binding site I of cTnC is inactive due to an amino acid insertion and several critical amino acid substitutions within the calcium-binding loop.

The consensus Ca^{2+}-binding loop of helix–loop–helix calcium-binding proteins consists of 12 sequential residues (Strynadka & James, 1989). Residues at positions 1, 3, 5, 7, and 12 of the loop coordinate the Ca^{2+} ion, with residue 12 providing bidentate coordination through both side-chain carboxylate oxygens (Figure 1). Thus, the Ca^{2+} ion is coordinated by seven ligands in a pentagonal bipyramidal geometry. Positions 1, 6, and 12 of the loop are invariably Asp, Gly, and Glu, respectively (Strynadka & James, 1989). In

† This work was supported in part by National Institutes of Health Grants GM41232 to P.R.R. and AR39218 to J.A.P., by a grant from the Robert Welch Foundation to J.A.P., and by Robert Welch foundation Grant C-1041 to Frederick B. Rudolph for support of R.M.M.B. J.A.P. is the recipient of a Career Research Development Award from the NIH.
* Author to whom correspondence should be addressed.

[1] Abbreviations: TnC, cardiac or fast skeletal troponin C; cTnC, cardiac TnC; sTnC, skeletal TnC; cTnC3, bacterially synthesized cTnC(desM1,D2A); CBM-IIA, cTnC3(D65A); EDTA, ethylenediaminetetraacetic acid; CDTA, *trans*-1,2-diaminocyclohexane-*N*,*N*,*N*′,*N*′-tetraacetic acid; DTT, 1,4-dithiothreitol; NMR, nuclear magnetic resonance; NOESY, two-dimensional proton nuclear Overhauser enhancement spectroscopy; NOE, nuclear Overhauser effect; HSMQC, heteronuclear single- and multiple-quantum shift correlation spectroscopy; NOESY-HMQC, three-dimensional nuclear Overhauser enhancement ^{15}N–^{1}H multiple-quantum coherence; 2D, two dimensional; 3D, three dimensional.

0006-2960/92/0431-1595$03.00/0

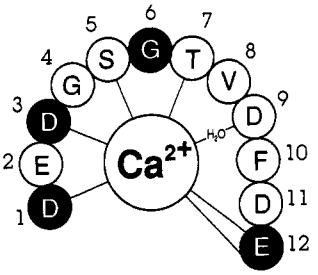

FIGURE 1: Schematic diagram of Ca^{2+}-binding loop II in cTnC. Shaded residues are highly conserved or invariant in all known helix–loop–helix Ca^{2+}-binding sites. Solid lines show the amino acid residues coordinating the Ca^{2+} ion.

all crystal structures of helix–loop–helix Ca^{2+}-binding proteins, the amide proton of the invariant Gly in position 6 forms a hydrogen bond with the side-chain carboxylate of Asp in position 1 (Strynadka & James, 1989).

Another distinctive feature of the helix–loop–helix Ca^{2+}-binding proteins is the short segment of antiparallel β-sheet formed between the two Ca^{2+}-binding loops in each domain. This interaction holds the Ca^{2+}-binding loops within each domain in close contact with each other and has been observed in the crystal structures of parvalbumin (Moews & Kretsinger, 1975), calmodulin (Babu et al., 1985), calbindin (Szebenyi & Moffat, 1986), and turkey and chicken fast skeletal TnC (Herzberg & James, 1988; Satyshur et al., 1988). These short β-sheets persist even in the N-terminal domain in the crystal structures of sTnC which do not have Ca^{2+} bound at sites I and II (Herzberg & James, 1988; Satyshur et al., 1988) and in the apo- form of calbindin (Szebenyi & Moffat, 1986). In addition, NMR has been used to study this interaction in solution in calmodulin (Ikura et al., 1987), parvalbumin (Padilla et al., 1990), calbindin (Drakenberg et al., 1989; Skelton et al., 1990), sTnC (Tsuda et al., 1988), and cTnC (Brito et al., 1991). Downfield-shifted CαH resonances and CαH–CαH NOEs were used to demonstrate the presence of adjacent β-strands in both the N- and C-terminal domains of Ca^{2+}-saturated cTnC3 and CBM-IIA (Brito et al., 1991). On the basis of these criteria, the short adjacent β-strands in the N-terminal domain of cTnC3 exist in solution even in the absence of Ca^{2+} at both sites I and II (Brito et al., 1991).

Nuclear magnetic resonance (NMR) provides a powerful approach for analyzing structure/function relationships in biological molecules. Recently, triple-resonance multidimensional NMR in combination with $^{13}C/^{15}N$ double labeling of proteins has greatly simplified the assignment of NMR signals and extended the molecular weight range accessible to NMR spectroscopy (Ikura et al., 1990a,b; Bax et al., 1990; Clore et al., 1990; Pelton et al., 1991a,b). With regard to helix–loop–helix Ca^{2+}-binding proteins, these techniques have been successfully applied to the study of calmodulin (Ikura et al., 1990b) and calmodulin complexed with the binding domain of skeletal muscle myosin light-chain kinase (Ikura et al., 1991).

To further explore conformational changes induced in cTnC upon Ca^{2+} binding, multidimensional NMR and isotope labeling of cTnC3 with ^{15}N-enriched amino acids has been used to assign the downfield-shifted amide resonances. The three most downfield amide resonances in the ^1H NMR spectrum of Ca^{2+}-saturated cTnC3 were assigned to the invariant glycine residues at position 6 of calcium-binding loops II, III, and IV, suggesting that these amides are involved in hydrogen bonding. No downfield-shifted Gly residue from site I was observed. Comparison of downfield-shifted amide protons in the Ca^{2+}-saturated forms of cTnC3 and CBM-IIA demonstrated that Gly70 is hydrogen bonded to the carboxylate side chain of Asp65. In the apo- form of cTnC3, only Gly70 was found to be shifted significantly downfield with respect to the remaining amide proton resonances. Thus, even in the absence of Ca^{2+} at binding site II, the amide proton of Gly70 is strongly hydrogen bonded to the side-chain carboxylate of Asp65.

The amide protons of Ile112 and Ile148 in the C-terminal domain and Ile36 in the N-terminal domain β-strands exhibit chemical shifts consistent with hydrogen-bond formation between the pair of Ca^{2+}-binding loops in each domain of Ca^{2+}-saturated cTnC3. In solution, the Ca^{2+}-saturated form of cTnC3 shows two strong hydrogen bonds stabilizing the β-sheet in the C-terminal domain but only one strong hydrogen bond in the β-sheet of the N-terminal domain.

Materials and Methods

Materials. $[^{15}N](NH_4)_2SO_4$ was obtained from EG&G Mound Applied Technologies. [^{15}N]Gly, [^{15}N]Leu, and [^{15}N]Phe were obtained from Isotec Inc. Deuterated algal amino acid mixture (98% deuterated) was obtained from MSD Isotopes. DEAE-Sepharose, Sephacryl S-100, and Phenyl-Sepharose were obtained from Pharmacia Chemicals. Deuterium oxide and Tris-d_{11} were purchased from Cambridge Isotope Labs. All other chemicals were of the highest purity available commercially.

Labeled Recombinant Proteins. Recombinant cardiac troponin C proteins were overexpressed in *Escherichia coli* JM109 and purified as previously described by Putkey et al. (1989) with the exception that the host cells were the JM109 strain of *E. coli* which had been transfected with the plasmid pGp1-2 which encodes a temperature sensitive λ repressor. Uniformly ^{15}N-enriched cTnC3 was obtained by growing the bacteria in M9 minimal medium [7 g of Na_2HPO_4, 3 g of KH_2PO_4, 0.5 g NaCl, 10 mL of 20% glucose, 1 mL of 1% thiamin, 0.1 mL of $CaCl_2$, 1 mL of 1 M $MgSO_4$, and 0.3 mL of 0.01 M $FeCl_3$ and 1 g of $(^{15}NH_4)_2SO_4$ per liter as the sole nitrogen source] supplemented with 50 mg/L ampicillin and 30 mg/L kanamycin. Selective ^{15}N-labeling of cTnC3 was achieved by growing the cells in M9 minimal medium supplemented with the ^{15}N-labeled amino acid and a mixture of the remaining 19 unlabeled amino acids (Muchmore et al., 1989). Random fractionally deuterated cTnC3 was prepared by growing the bacteria in M9 minimal medium supplemented with a mixture of deuterated algal amino acids (0.6 g/L).

Protein samples for NMR experiments were extensively dialyzed against 50 mM $(NH_4)HCO_3$, lyophilized, and dissolved in NMR buffer containing 20 mM Tris-d_{11} and 200 mM KCl in 90% H_2O and 10% ^2H_2O at pH 6.0. All buffer and reagent solutions used in the NMR studies were treated with Chelex 100 before use to remove trace metal contaminants. For preparation of apoproteins, samples were made 5–10 mM in both CDTA and EDTA, and approximately 1 $\times$ 10^5 cpm of $^{45}Ca^{2+}$ was added. The proteins were then desalted on a Bio-Gel P-6DG (Bio-Rad) column equilibrated in Chelex treated 10 mM $(NH_4)HCO_3$ buffer, pH 7.5. Protein fractions devoid of $^{45}Ca^{2+}$ were pooled, lyophilized, and dissolved in the NMR buffer described above. Just prior to the NMR experiments, DTT was added to the samples in a 5-fold molar excess over protein (cTnC3 and CBM-IIA). Final protein concentrations varied from 1.5 to 3 mM.

NMR Methods. Heteronuclear single- and multiple-quantum coherence (HSMQC) (Zuiderweg, 1990) spectra of the ^{15}N-labeled proteins were collected with 1024 complex data points in the t_2 domain and 350 increments in t_1. The ^1H and ^{15}N spectral widths were 7142 and 4000 Hz, respectively. The water resonance was suppressed by continuous irradiation

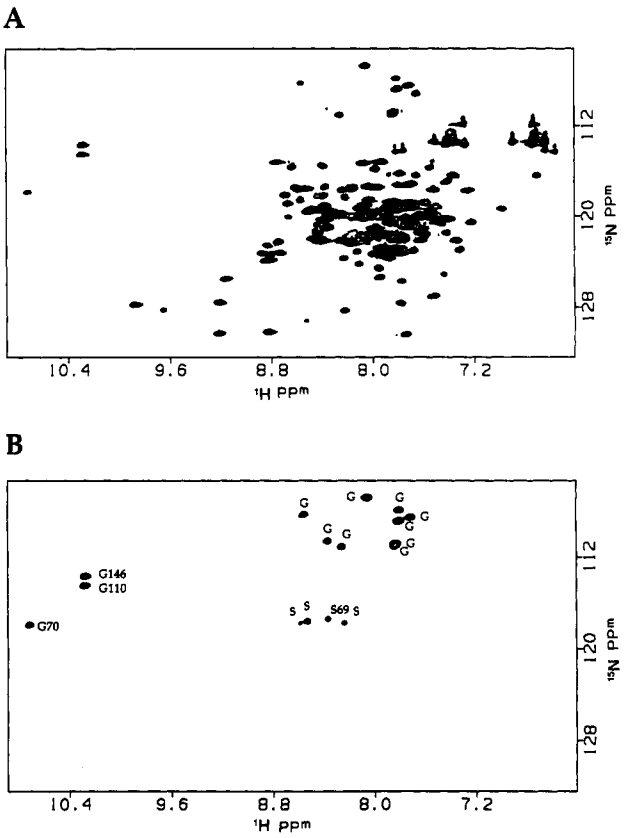

FIGURE 2: Heteronuclear multiple-quantum ^{1}H–^{15}N shift correlation spectra of Ca^{2+}-saturated cTnC3 uniformly labeled with ^{15}N (A) and selectively labeled with [^{15}N]Gly and [^{15}N]Ser (B). Samples were approximately 1.6 mM cTnC3 in 20 mM Tris-d_{11}, 200 mM KCl, and 8 mM DTT in 90% H_2O/10% ^2H_2O at pH 6.0. Spectra were obtained at 500 MHz and 40 °C as described under Materials and Methods.

during the relaxation delay. HSMQC spectra were processed with a Gaussian multiplication and an exponential multiplication with a negative time constant in t_2 and with a 45°-shifted sine-bell function in t_1 and zero-filled to 1024 and 2048 real data points in t_1 and t_2, respectively. Phase-sensitive NOESY spectra (States et al., 1982; Macura et al., 1982) were collected with a 300-ms mixing time as 256 t_1 × 1024 t_2 complex data points, a spectral width of 7142 Hz in both dimensions, and 32 scans per t_1. NOESY spectra were processed with a 45°-shifted skewed sine-bell squared function in t_2 and a 45°-shifted sine-bell function in t_1, and zero-filled to 2048 × 2048 points. The three-dimensional NOESY-HMQC spectrum was obtained as described by Kay et al. (1989) with continuous irradiation of the H_2O resonance during the relaxation delay and ^{15}N decoupling during acquisition. A total of 128 complex t_1 (^{1}H), 32 complex t_2 (^{15}N), and 1024 complex t_3 (^{1}H) data points were collected. Spectral widths in the F_1 and F_3 dimensions were 6250 Hz, while the F_2 spectral width was 1538 Hz. The delay Δ was set to 4.5 ms which is slightly less than $1/2J_{NH}$. The 3D NOESY-HMQC was processed with a 45°-shifted sine-bell weighting function in all dimensions and zero filling in each dimension to obtain a final absorptive matrix of 512 × 64 × 512 of real data points. ^{1}H and ^{15}N chemical shifts were reported relative to the HDO signal at 4.563 ppm and $^{15}NH_4Cl$ in 1 M HCl at 25.2 ppm, respectively. All spectra were processed using the FELIX software package (Hare Research, Inc.).

Results

Uniform and selective ^{15}N labeling of recombinant cTnC, cTnC3, has been used to aid in sequential resonance assignment of the downfield-shifted amide protons. Selective labeling of cTnC3 with [^{15}N]Gly permitted several entry points for sequence-specific assignment. Metabolic interconversion between glycine and serine resulted in partial incorporation of [^{15}N]Gly into [^{15}N]Ser. The ^{1}H–^{15}N correlation maps of Ca^{2+}-saturated uniformly ^{15}N-enriched cTnC3 and [^{15}N]-Gly-,Ser-labeled cTnC3 are shown in Figure 2, panels A and B, respectively. On the basis of the amino acid composition of bacterially synthesized cTnC3, 176 cross-peaks were expected in the HSMQC spectrum of uniformly ^{15}N-labeled cTnC3. At least 151 of the expected 176 cross-peaks were resolved (Figure 2A), demonstrating the feasibility of and providing a master template for sequence-specific assignment of cTnC3. All 12 Gly and four Ser residues could be resolved in the selectively [^{15}N]Gly-,Ser-labeled sample of Ca^{2+}-saturated cTnC3 (Figure 2B). Serine ^{1}H–^{15}N correlations were distinguished from ^{1}H–^{15}N Gly correlations on the basis of their observed ^{15}N chemical shifts (Glushka et al., 1990) and the lower intensity of the Ser cross-peaks compared to those of Gly (Ikura et al., 1990a). Comparison of Figure 2 panels A and B shows that the three most downfield-shifted amide proton resonances belong to Gly residues. The most downfield-shifted amide proton at 10.68 ppm was assigned to Gly70 on the basis of a sequential NOE to a Ser residue at 8.36 ppm (Figure 3; Table I), assigned from the HSMQC spectrum of [^{15}N]Gly-,Ser-labeled cTnC3 (Figure 2B). The only Ser–Gly dipeptide in cTnC3 is Ser69–Gly70, located in Ca^{2+}-binding site II of cTnC3. The amide resonance at 10.68 ppm also has a strong NOE to an amide resonance at 7.79 ppm (Figure 3), permitting assignment of this resonance to Thr71 (Table I). However, chemical shift degeneracy of the amide protons in the 2D NOESY spectrum prevented further extension of this stretch of sequential NOE connectivities.

The HSMQC spectrum of [^{15}N]Gly-,Ser-labeled cTnC3 shows two downfield-shifted Gly residues having degenerate proton chemical shifts at 10.26 ppm (Figure 2B). The NOESY spectrum of cTnC3 showed four strong NH(i)–NH(i+1) and two NH to aromatic NOEs to the degenerate Gly protons at 10.26 ppm (Figure 3). The aromatic resonances were previously assigned to C3,5H of Phe101 and C2,6H of Tyr111, respectively (Brito et al., 1991). The amide proton resonance at 9.87 ppm also showed NOEs to the C4H and C2,6H aromatic protons of Phe101 and Tyr111, respectively. In addition, sequential NOEs were observed from amide protons at 9.87 and 10.26 ppm to an amide proton at 7.95 ppm in the NOESY spectrum of perdeuterated cTnC3 (Figure 3B). Selectively [^{15}N]Leu-, Ile-labeled cTnC3 established that the amide proton at 9.87 ppm was an Ile (Figure 5C). From the primary sequence, this stretch of sequential NOEs must correspond to Gly110–Tyr111–Ile112. NOEs from the amide

Table I: ^{1}H and ^{15}N Chemical Shift Assignments for Ca^{2+}-Saturated cTnC3 at 40 °C and pH 6.0[a]

residue	NH	^{15}N	residue	NH	^{15}N
I36	9.60	127.4	D145	8.49	
			G146	10.26	114.6
S69	8.36	117.4	R147	7.69	
G70	10.68	118.1	I148	9.20	127.6
T71	7.79		D149	9.21	
V72	8.51				
			E152	8.73	
D109	8.40		F153	9.13	125.5
G110	10.26	113.2	L154	8.10	120.1
Y111	7.95				
I112	9.87	127.8			
D113	8.82				

[a] ^{1}H and ^{15}N chemical shifts are reported relative to the HDO signal at 4.563 ppm and $^{15}NH_4Cl$ in 1 M HCl at 25.2 ppm, respectively.

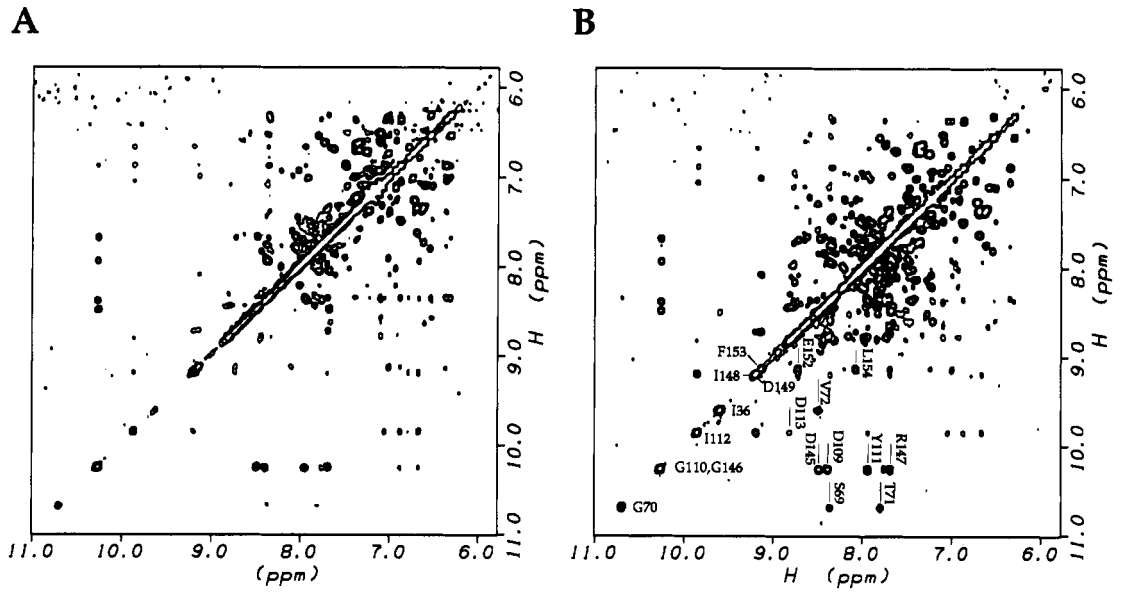

FIGURE 3: Downfield region of the 500-MHz phase-sensitive NOESY spectra of Ca^{2+}-saturated cTnC3 (A) and Ca^{2+}-saturated perdeuterated cTnC3 (B). The mixing times were 300 ms with continuous irradiation of the H_2O resonance during the delay. Both samples were 3 mM cTnC3 in 20 mM Tris-d_{11}, 200 mM KCl, and 15 mM DTT in 90% H_2O/10% ^2H_2O at pH 6.0 and 40 °C. Other parameters are given under Materials and Methods.

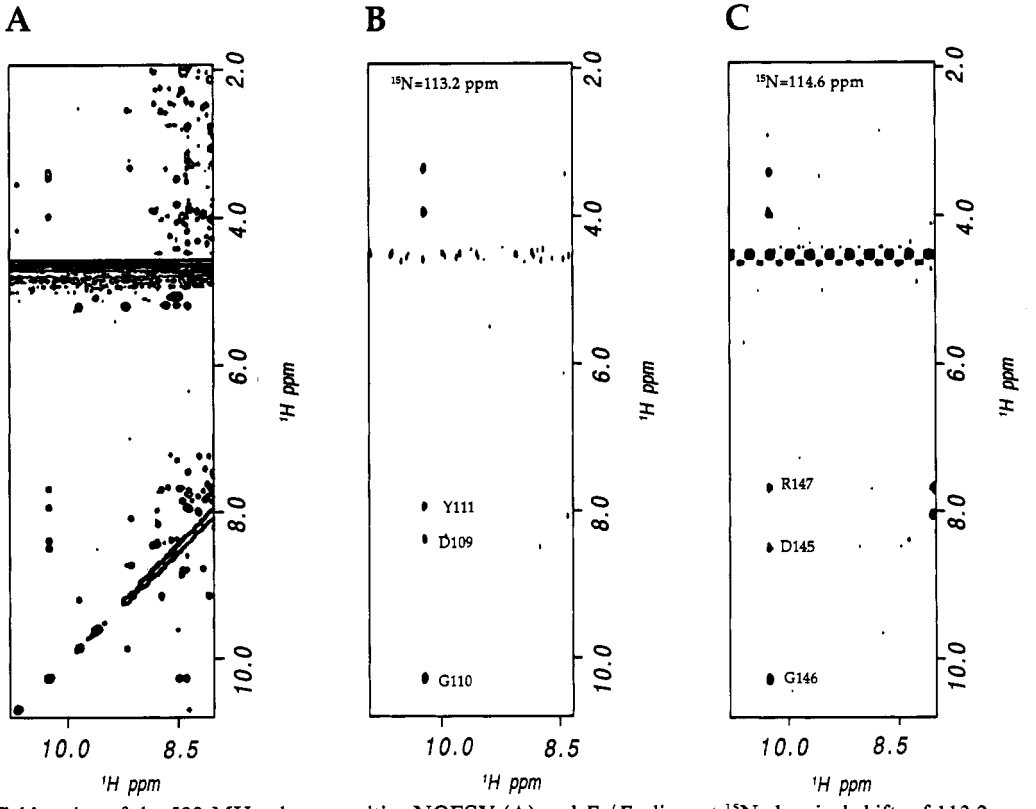

FIGURE 4: Downfield region of the 500-MHz phase-sensitive NOESY (A) and F_1/F_3 slices at ^{15}N chemical shifts of 113.2 ppm (B) and 114.6 ppm (C) from the NOESY-HMQC spectrum of Ca^{2+}-saturated uniformly ^{15}N-labeled cTnC3. Sample conditions are described in the legend to Figure 3. Data collection and processing for the 3D NOESY-HMQC are described under Materials and Methods.

protons of Gly110 and Ile112 to the aromatic ring of Tyr111 are also consistent with this assignment. Assignment of the Tyr111 NH was confirmed by NOEs to its own side-chain resonances.

In order to resolve the degenerate Gly amide protons, a 3D NOESY-HMQC spectrum was obtained on uniformly ^{15}N-enriched cTnC3. Figure 4 compares F_1/F_3 slices at ^{15}N chemical shifts of 113.2 and 114.6 ppm from the 3D NOESY-HMQC spectrum of uniformly enriched [^{15}N]cTnC3 with the 2D NOESY of unlabeled cTnC3. Both Gly NH resonances were resolved on the basis of their ^{15}N amide chemical shifts. NOE connectivities from the Gly amide in the F_1/F_3 slice at a ^{15}N chemical shift of 113.2 ppm to Asp109 and Tyr111 NH resonances permitted assignment of this amide to Gly110 (Figure 4B; Table I). Both Gly70 and Gly110 are the sixth ligands in Ca^{2+}-binding loops II and III, respectively. The remaining downfield-shifted amide having ^{1}H and ^{15}N chemical shifts of 10.26 and 114.6 ppm (Figure 4C; Table I), respectively, was assigned to Gly146, the sixth ligand in Ca^{2+}-binding loop IV. No downfield-shifted NH resonance was observed from Ca^{2+}-binding loop I. Sequential assignment from Asp145 to Asp149 and Glu152 to Leu154 in Ca^{2+}-

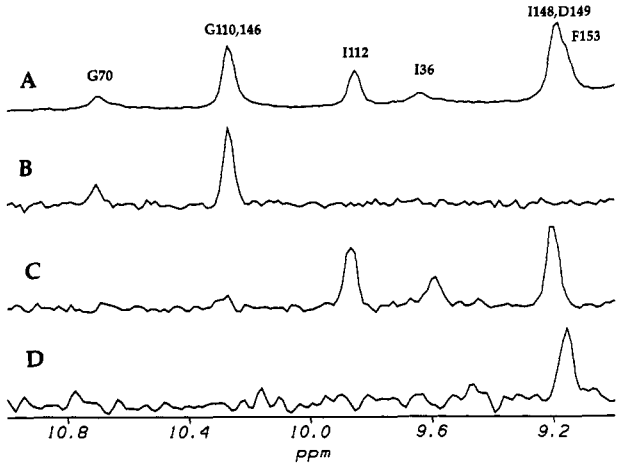

FIGURE 5: Downfield region of the ^1H NMR spectrum of Ca^{2+}-saturated cTnC3 (A) and the ^{15}N-edited spectra of selectively labeled ([^{15}N]Gly,Ser)cTnC3 (B), ([^{15}N]Leu,Ile)cTnC3 (C), and ([^{15}N]-Phe)cTnC3 (D). ^{15}N-edited spectra were obtained with ^{15}N decoupling during acquisition and continuous irradiation of the H_2O resonance during the delay. Other conditions are as described in the legend to Figure 2.

binding loop IV was possible using NH(i)–NH(i+1) and NH–CαH connectivities as well as selective ^{15}N-labeling of cTnC3 (Figures 3B, 4, and 5; Table I). A large NH–NH NOE was observed between amide resonances assigned to Ile112 and Ile148 (Figure 3). The magnitude of this NOE was greatly increased due to decreased spin diffusion in the perdeuterated cTnC3 sample (Figure 3B). Ile112 and Ile148 are located at the center of a short β-sheet formed between Ca^{2+}-binding loops III and IV in the model of cTnC (Figure 6; Brito et al., 1991) and the crystal structure of sTnC (Herzberg & James, 1988; Satyshur et al., 1988). Hydrogen bonds between the carbonyl and amide groups of these Ile residues are proposed to stabilize this short β-sheet.

Calcium titration of apo-cTnC3 was performed to monitor the effect of Ca^{2+} on the downfield-shifted amide protons assigned to calcium-binding loops II, III, and IV (Figure 7). In the absence of Ca^{2+}, only a single broad downfield-shifted amide proton was observed (Figure 7A). The addition of Ca^{2+} sufficient to fill high-affinity binding sites III and IV resulted in the appearance of amide resonances assigned to Gly110, Gly146, Ile112, Ile148, Asp149, and Phe153 (Figure 7B). Stepwise addition of Ca^{2+} up to a metal/cTnC3 ratio of 4 resulted in progressive downfield shifts of the amide protons of Gly70 and Ile36 (Figure 7C–E). Both Gly70 and Ile36 are located in the N-terminal domain of cTnC3. The assignment of Ile36 was confirmed by selective labeling (Figure 5C) and the presence of NOEs to the CαH of Cys35 (Brito et al., 1991) and to the amide proton of Val72 (Figure 3B). This NOE was not observable in the NOESY spectrum of unlabeled cTnC3 (Figure 3A). From the titration, the single downfield-shifted amide proton in apo-cTnC3 could be confidently assigned to Gly70 (Figure 7).

Inactivation of Ca^{2+}-binding site II in cTnC3 through mutation of Asp65 to Ala (CBM-IIA) has been shown to prevent the Ca^{2+}-dependent activation of muscle contraction by cTnC3 (Putkey et al., 1989). Mutation of Asp65 to Ala not only results in the loss of a Ca^{2+}-coordinating ligand but also potentially disrupts the hydrogen-bonding network thought to be responsible for maintaining the correct spatial orientation of the Ca^{2+}-binding loop. Comparison of the downfield-shifted amide region of the ^1H NMR spectra of Ca^{2+}-saturated CBM-IIA and cTnC3 showed that the amide proton resonances assigned to the C-terminal domain of cTnC3 were not perturbed by the mutation in site II (Figure 7E,F). However, the amide protons of Gly70 and Ile36 in Ca^{2+}-saturated CBM-IIA were not observed downfield of 9.00 ppm, indicating a loss of strong hydrogen bonds involving these amide protons (Figure 7E,F).

Discussion

Conformational changes induced in cTnC in response to Ca^{2+}-binding at site II are responsible for triggering muscle contraction. In an effort to better understand these changes, we have studied the downfield-shifted amide region of the ^1H NMR spectrum of recombinant cTnC3 and CBM-IIA, a mutant unable to bind Ca^{2+} at site II. Low-field amide proton chemical shifts have previously been correlated with the length of the hydrogen bond between the amide proton and the oxygen acceptor (Wagner et al., 1983). Amide proton chemical shifts above 9 ppm are generally considered diagnostic for strong hydrogen bonds (Wagner et al., 1983; Pardi et al., 1983). Downfield-shifted amide protons were assigned using stable isotope enrichment and heteronuclear multidimensional NMR (Figures 2–5). The most downfield-shifted amide proton resonances were assigned to Gly70, Gly110, and

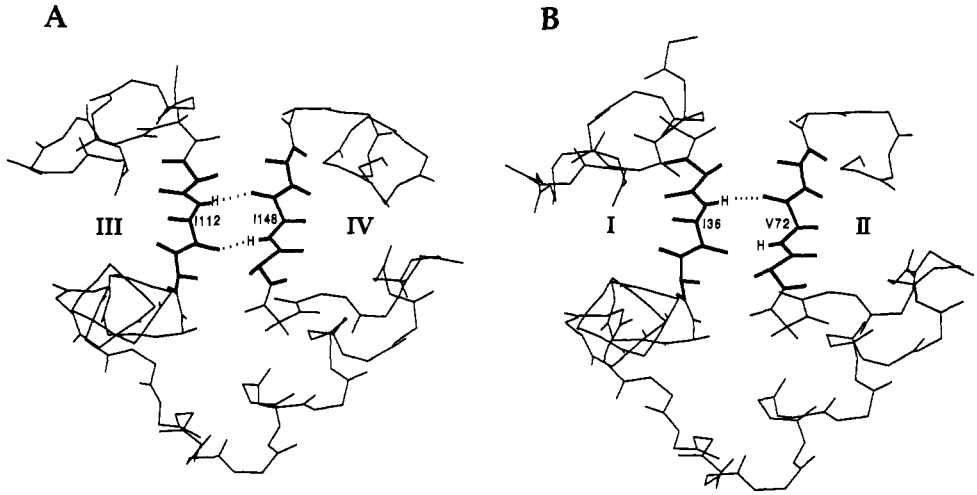

FIGURE 6: Views of the proposed β-sheet structures in cTnC3 based on the crystal structure of sTnC (Herzberg & James, 1988) and the model of cTnC (Brito et al., 1991). The β-sheet between Ca^{2+}-binding loops III and IV in the C-terminal domain of cTnC3 is shown in panel A. The β-sheet between Ca^{2+}-binding loops I and II in the N-terminal domain of cTnC3 is shown in panel B. Location of the β-strands in solution is shown as thick lines. Hydrogen bonds that can be assigned on the basis of NMR data are shown with dotted lines.

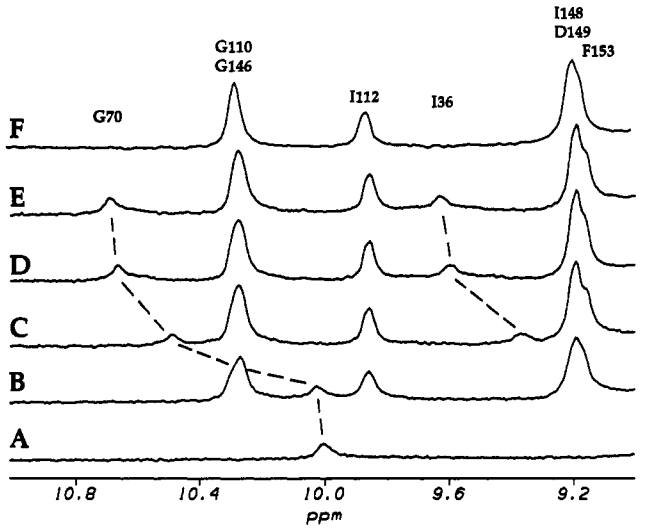

FIGURE 7: Calcium titration of cTnC3 monitoring the downfield amide proton region of the ^1H NMR spectrum. The Ca^{2+}/protein ratios shown were 0 (A), 2 (B), 2.5 (C), 3 (D), and 4 (E). The downfield-shifted amide proton region of the ^1H NMR spectrum of Ca^{2+}-saturated CBM-IIA is shown in panel F. The samples contained 1.0 mM protein in 20 mM Tris-d_{11}, 200 mM KCl, and 5 mM DTT in 90% H_2O/10% ^2H_2O at pH 6.0 and 40 °C.

Gly146. These Gly residues are located in the 6th position of Ca^{2+}-binding loops II, III, and IV, respectively, in cTnC3 (Figure 1; Table I). No downfield-shifted Gly amide resonance was found for the naturally inactive Ca^{2+}-binding loop I. An extended network of hydrogen bonds is responsible for maintaining the structural integrity of the Ca^{2+}-binding loop (Strynadka & James, 1989). Amide protons of glycine residues located in the 6th position of Ca^{2+}-binding loops I–IV in calmodulin (Ikura et al., 1987, 1990b), loops III and IV in sTnC (Tsuda et al., 1988, 1990), a polypeptide dimer comprising the fourth Ca^{2+}-binding site of sTnC (Kay et al., 1991), and loop II in calbindin D_{9k} (Kordel et al., 1989) have also been shown to have unusual downfield chemical shifts.

The origin of these unusual chemical shifts was suggested to result from hydrogen bond formation with the side-chain carboxylate group of the invariant Asp residue located in position 1 of the EF-hand Ca^{2+}-binding loops (Ikura et al., 1987). However, the hydrogen-bond acceptor was not identified in solution. Comparison of the downfield-shifted amide protons in Ca^{2+}-saturated cTnC3 and CBM-IIA shows that in the absence of a carboxylate side chain in position 1 of Ca^{2+}-binding loop II, the amide resonance of Gly70 is not shifted significantly downfield (Figure 7E,F). These results suggest the downfield chemical shift of the Gly70 amide proton is due to hydrogen bonding with the carboxylate side chain of Asp65. This provides the first direct demonstration that in solution the Gly amide at position 6 is hydrogen bonded with the carboxylate side chain of Asp at position 1 in Ca^{2+}-binding site II. Thus in Ca^{2+}-saturated cTnC3, Gly110 and Gly146 are most likely hydrogen bonded to the carboxylate side chains of Asp105 and Asp141 in sites III and IV, respectively. As expected, no downfield-shifted amide resonance was observed from the inactive site I since this site contains an insertion and several amino acid substitutions which eliminates the normal hydrogen-bond acceptor.

In the apo- form of cTnC3, only a single downfield-shifted amide proton (10.0 ppm) was observed (Figure 7A). Titration of the apo- form of cTnC3 with Ca^{2+} while monitoring the downfield-shifted amide region of the ^1H NMR spectrum permitted assignment of this resonance to Gly70 (Figure 7). Thus, even in the absence of bound Ca^{2+} at site II, the backbone amide of Gly70 is hydrogen bonded, albeit weaker, with the carboxylate side chain of Asp65. The amide protons of Gly32 and Gly68 in apo-sTnC were also found to resonant at low fields, suggesting hydrogen-bond formation with Asp residues at position 1 in sites I and II (Tsuda et al., 1990).

In contrast to what is observed in site II, the amide protons of Gly110 and Gly146 of sites III and IV do not appear to form hydrogen bonds, or do so weakly, until Ca^{2+} binds (Figure 7). Consistent with this observation, the Gly residues in sites III and IV in the C-terminal domain of sTnC also do not form hydrogen bonds in the absence of Ca^{2+} (Tsuda et al., 1988). In contrast, Gly residues at position 6 in Ca^{2+}-binding loops I, II, and III of calmodulin were judged to form hydrogen bonds in the absence of bound Ca^{2+} on the basis of the chemical shifts of the amide protons (Ikura et al., 1987). However, the Gly in site IV of calmodulin was not found to form a hydrogen bond detectable by NMR until metal binds. These results may suggest structural differences between the Ca^{2+}-binding domains of troponin C (skeletal and cardiac) and calmodulin.

The remaining downfield-shifted amide protons were assigned to Ile36 in the N-terminal domain and Ile112, Ile148, Phe153, and Asp149 in the C-terminal domain of cTnC3, respectively (Figures 2–5; Table I). Isoleucines -36, -112, and -148 are located in short β-sheet structures between helix–loop–helix Ca^{2+}-binding sites in both the N- and C-terminal domains. Short β-sheet structures between Ca^{2+}-binding loops have been observed in the crystal structures of sTnC (Herzberg & James, 1985, 1988; Herzberg et al., 1986; Sundaralingam et al., 1985; Satyshur et al., 1988). As a consequence of the unique CαH chemical shifts of residues located in β-sheet structures, NMR has been used to study these structures in sTnC (Tsuda et al., 1988) and in both normal, cTnC3, and mutant, CBM-IIA, cardiac troponin C (Brito et al., 1991). From chemical shifts (Table I) and the pattern of interresidue NOEs, the β-sheet between Ca^{2+}-binding sites III and IV are formed by Tyr111–Ile112–Asp113 and Arg147–Ile148–Asp149, respectively (Figure 6A; Brito et al., 1991).

Titration of apo-cTnC3 with Ca^{2+} sufficient to fill high-affinity sites III and IV (Figure 7B) resulted in downfield shifts of the amide proton resonances of Ile112, Ile148, Asp149, and Phe 153. The amide of Ile112 forms a hydrogen bond upon the addition of Ca^{2+} with the carbonyl of Ile148 the most likely hydrogen-bond acceptor (Figure 6A). The downfield shift of the Ile148 amide proton is also consistent with hydrogen-bond formation with the carbonyl of Ile112 (Figure 6A). From the model of cTnC (Brito et al., 1991), both of these residues are at the center of the β-sheet formed between Ca^{2+}-binding loops III and IV. In support of this, a strong interstrand NH–NH NOE was observed between Ile112 and Ile148 (Figure 3B). This is also consistent with the crystal structure (Herzberg & James, 1988) and solution data (Tsuda et al., 1988) on sTnC. In apo-cTnC, no tight hydrogen bonds were detected between Ile112 and Ile148 based on the absence of low-field shifts for these amide protons (Figure 7A). These data suggest that, in the absence of Ca^{2+}, the short β-sheet between Ca^{2+}-binding sites III and IV is either disrupted or significantly weakened.

Previous studies have suggested that Thr71–Val72–Asp73 in Ca^{2+}-binding loop II and Cys35–Ile36–Ser37 in the naturally inactive Ca^{2+}-binding loop I form β-strands in both the presence and absence of Ca^{2+} (Figure 6B; Brito et al., 1991). In support of this, an NOE was observed between the amide protons of Ile36 and Val72 in Ca^{2+} saturated cTnC3 (Figure 3B). Ile36 is at the center of the β-sheet between Ca^{2+}-binding

loops I and II and is presumably hydrogen bonded to Val72 (Figure 6B). Progressive addition of Ca^{2+} sufficient to fill site II resulted in the downfield shift of the Ile36 amide proton resonance, suggesting hydrogen bond formation upon Ca^{2+} binding at site II (Figure 7). Inactivation of Ca^{2+}-binding site II (CBM-IIA), by conversion of Asp65 to Ala, results in the loss or weakening of this hydrogen bond since no downfield chemical shift is observed for this resonance (Figure 7F). The amide proton of Ile36 is also not significantly downfield shifted in cTnC3 having Ca^{2+} bound only at sites III and IV (Figure 7B). The amide proton resonance of Val72, at position 8 in binding site II, was found not to be significantly shifted downfield (8.51 ppm; Figure 3B). In contrast, Ile148 in position 8 of loop IV in the C-terminal domain was shown to be involved in a strong hydrogen bond with Ile112 (Figures 6A and 7). Therefore, on the basis of low-field shifted amide proton resonances in Ca^{2+}-saturated cTnC3, the N- and C-terminal domains were found to have one and two tight interstrand hydrogen bonds, respectively. These results are consistent with the formation of a short β-sheet between loops I and II of Ca^{2+}-saturated cTnC3 which appears to be less stable than the β-sheet observed in the C-terminal domain between loops III and IV. However, it should be remembered that large downfield shifts from the random coil values of the amide protons are expected only for hydrogen-bond distances of <2 Å between the hydrogen and acceptor atoms (Wagner et al., 1983). The crystal structure of sTnC, which does not have Ca^{2+} bound at sites I and II, shows four interstrand hydrogen bonds in the N-terminal β-sheet, but these are weaker than the two hydrogen bonds observed in the β-sheet of the Ca^{2+}-saturated C-terminal domain (Herzberg & James, 1988; Strynadka & James, 1989). In addition, loops I and II in sTnC show more conformational flexibility than loops III and IV as judged by the crystallographic temperature factors (B values) (Herzberg & James, 1988).

Comparison of the N-terminal domains in sTnC and cTnC suggests possible differences in the orientation and/or flexibility of the short β-sheet between Ca^{2+}-binding loops I and II. In apo-cTnC3 no tight hydrogen bonds were observed between residues assigned to the short β-strands in the N-terminal domain (Figure 7). However, Ile70 in apo-skeletal TnC, corresponding to Val72 in cTnC3, was found to resonate at low field, indicating the formation of a hydrogen bond between the β-strands in the N-terminal domain even in the absence of bound Ca^{2+} (Tsuda et al., 1988). In contrast, no tight hydrogen bonds were observed in the N-terminal β-sheet of Ca^{2+} saturated sTnC, as judged from the lack of downfield-shifted amides (Tsuda et al., 1988). Sequence-specific assignment has permitted us to detect one tight hydrogen bond between β-strands in the N-terminal domain of Ca^{2+}-saturated cTnC3, suggesting differences in the flexibility and orientation of the β-sheet structure in Ca^{2+}-loaded sTnC and cTnC. It is possible that the flexibility and/or orientation of the β-sheet and Ca^{2+}-binding loop structures in the N-terminal half of TnC contribute to the metal-dependent contractile properties of different muscle types. For example, the Ca^{2+} and Sr^{2+} sensitivities of cardiac and slow skeletal muscle fibers appear solely dependent on the isoform of TnC (Hoar et al., 1988; Babu et al., 1987; Morimoto et al., 1988; Sweeney et al., 1990), while, in fast skeletal muscle fibers, specific interactions between sTnC and other troponin subunits also contribute to Sr^{2+} sensitivity (Kerrick et al., 1985; Hoar et al., 1988; Morimoto et al., 1988). Structural features of TnC that may be important for differential interaction with isoforms of troponin I and/or T may be encoded by domain I since an active site I alone in the N-terminus of a recombinant form of cTnC cannot regulate contraction in slow muscle fibers (Sweeney et al., 1990), while the same protein, and an analogous recombinant derivative of sTnC, can support partial contraction in fast skeletal muscle fibers (Putkey et al., 1991; Sheng et al., 1990). Studies are currently in progress using stable isotope enrichment and multidimensional NMR to more fully characterize, at the molecular level, the Ca^{2+}-dependent conformational changes in TnC that regulate muscle contraction and how these changes differ between the cardiac and skeletal isoforms.

In summary, isotope labeling and multidimensional NMR have permitted unequivocal assignment of the downfield-shifted amide protons in recombinant cardiac TnC. Our results suggest that a hydrogen bond is present between the amide of Gly70 and the carboxylate side chain of Asp65 even in the absence of bound Ca^{2+} in the N-terminal domain of cTnC3. The binding of Ca^{2+} at site II tightens the Ca^{2+}-binding loop causing a reorientation or decrease in flexibility in the N-terminal domain β-sheet as detected by the formation or strengthening of the hydrogen bond between Ile36 amide and Val72 carbonyl. These conformational changes could then be responsible for the relative movement of helices B and C with respect to helices A and D, resulting in exposure of a hydrophobic surface as proposed by Herzberg and James (1986). The interaction of this hydrophobic surface with the other components of the troponin complex is thought to provide the critical change responsible for initiating muscle contraction.

Registry No. Asp, 56-84-8; Gly, 56-40-6; Ile, 73-32-5; Ca^{2+}, 7440-70-2.

References

Babu, A., Scordilis, S. P., Sonnenblick, E. H., & Gulati, J. (1987) *J. Biol. Chem. 262*, 5815.

Babu, Y. S., Bugg, C. E., & Cook, W. J. (1988) *J. Mol. Biol. 203*, 191.

Bax, A., Clore, G. M., Driscoll, P. C., Gronenborn, A. M., Ikura, M., & Kay, L. E. (1988) *J. Magn. Reson. 87*, 620.

Brenner, B. (1989) in *Molecular Mechanisms in Muscle Contraction* (Squire, J. M., Ed.) pp 76–149, CRC Press, Boca Raton, FL.

Brito, R. M. M., Putkey, J. A., Strynadka, N. C. J., James, M. N. G., & Rosevear, P. R. (1991) *Biochemistry 30*, 10236.

Cachia, P. J., Sykes, B. D., & Hodges, R. S. (1983) *Biochemistry 22*, 4145.

Clore, M. G., Bax, A., Driscoll, P. C., Wingfield, P. T., & Gronenborn, A. M. (1990) *Biochemistry 29*, 8172.

Collins, J. H., Greaser, M. L., Potter, J. D., & Horn, M. J. (1977) *J. Biol. Chem. 252*, 6356.

Drakenberg, T., Hofman, T., & Chazin, W. J. (1989) *Biochemistry 28*, 5946.

Glushka, J., Lee, M., Coffin, S., & Cowburn, D. (1990) *J. Am. Chem. Soc. 112*, 2843.

Herzberg, O., & James, M. N. G. (1985) *Nature 313*, 653.

Herzberg, O., & James, M. N. G. (1988) *J. Mol. Biol. 203*, 761.

Herzberg, O., Moult, J., & James, M. N. G. (1986) *J. Biol. Chem. 261*, 2638.

Hoar, P. E., Potter, J. D., & Kerrick, W. G. L. (1988) *J. Muscle Res. Cell Motil. 9*, 165.

Holroyde, M. J., Robertson, S. P., Johnson, J. D., Solaro, R. J., & Potter, J. D. (1980) *J. Biol. Chem. 255*, 11688.

Ikura, M., Minowa, O., & Hikichi, K. (1985) *Biochemistry 24*, 4264.

Ikura, M., Minowa, O., Yazawa, M., Yagi, K., & Hikichi,

K. (1987) *FEBS Lett. 219*, 17.
Ikura, M., Krinks, M., Torchia, D. A., & Bax, A. (1990a) *FEBS Lett. 266*, 155.
Ikura, M., Kay, L. E., & Bax, A. (1990b) *Biochemistry 29*, 4659.
Ikura, M., Kay, L. E., & Bax, A. (1991) *Biochemistry 30*, 5498.
Johnson, J. D., Collins, J. H., Robertson, S. P., & Potter, J. D. (1980) *J. Biol. Chem. 255*, 9635.
Kay, L. E., Marion, D., & Bax, A. (1989) *J. Magn. Reson. 84*, 72.
Kay, L. E., Forman-Kay, J. D., McCubbin, W. D., & Kay, C. M. (1991) *Biochemistry 30*, 4323.
Kerrick, W. G., Zot, H. G., Hoar, P. E., & Potter, J. D. (1985) *J. Biol. Chem. 260*, 15687.
Kördel, J., Forsén, S., & Chazin, W. J. (1989) *Biochemistry 28*, 7065.
Macura, S., Wüthrich, K., & Ernst, R. R. (1982) *J. Magn. Reson. 47*, 351.
Moews, P. C., & Kretsinger, R. H. (1975) *J. Mol. Biol. 91*, 201.
Morimoto, S., & Ohtsuki, I. (1988) *J. Biochem. (Tokyo) 104*, 149.
Muchmore, D. C., McIntosh, L. P., Russel, C. B., Anderson, D. E., & Dahlquist, F. W. (1989) *Methods Enzymol. 177*, 44.
Padilla, A., Vuister, G. W., Boelens, R., Kleywegt, G. J., Cave, A., Parello, J., & Kaptein, R. (1990) *J. Am. Chem. Soc. 112*, 5024.
Pardi, A., Wagner, G., & Wüthrich, K. (1983) *Eur. J. Biochem. 137*, 445.
Pelton, J. G., Torchia, D. A., Meadow, N. D., Wong, C.-Y., & Roseman, S. (1991a) *Proc. Natl. Acad. Sci. U.S.A. 88*, 3479.
Pelton, J. G., Torchia, D. A., Meadow, N. D., Wong, C.-Y., & Roseman, S. (1991b) *Biochemistry 30*, 10043.
Potter, J. D., & Gergely, J. (1977) *J. Biol. Chem. 250*, 34628.
Putkey, J. A., Sweeney, H. L., & Campbell, S. T. (1989) *J. Biol. Chem. 264*, 12370.
Putkey, J. A., Lui, W., & Sweeney, H. L. (1991) *J. Biol. Chem. 266*, 14881.
Satyshur, K. A., Rao, S. T., Pyzalska, D., Drendel, W., Greaser, M., & Sundaralingam, M. (1988) *J. Biol. Chem. 263*, 1628.
Sheng, Z., Strauss, W. L., Francois, J. M., & Potter, J. D. (1990) *J. Biol. Chem. 265*, 21554.
Skelton, N. J., Kördel, J., Forsén, S., & Chazin, W. J. (1990) *J. Mol. Biol. 213*, 593.
States, D. J., Haberkorn, R. A., & Ruben, D. J. (1982) *J. Magn. Reson. 48*, 286.
Strynadka, N. C. J., & James, M. N. G. (1989) *Annu. Rev. Biochem. 58*, 951.
Sundaralingam, M., Bergstrom, R., Strasburg, G., Rao, S. T., Roychowdhury, P., Greaser, M., & Wang, B. C. (1985) *Science 227*, 945.
Sweeney, H. L., Brito, R. M. M., Rosevear, P. R., & Putkey, J. A. (1990) *Proc. Natl. Acad. Sci. U.S.A. 87*, 9538.
Szebenyi, D. M. E., & Moffat, K. (1986) *J. Biol. Chem. 261*, 8761.
Tsuda, S., Hasegawa, Y., Yoshida, M., Yagi, K., & Hikichi, K. (1988) *Biochemistry 27*, 4120.
Tsuda, S., Ogura, K., Hasegawa, Y., Yagi, K., & Hikichi, K. (1990) *Biochemistry 29*, 4951.
Wagner, G., Pardi, A., & Wuthrich, K. (1983) *J. Am. Chem. Soc. 104*, 3731.
Van Eerd, J. P., & Takahashi, K. (1975) *Biochem. Biophys. Res. Commun. 64*, 122.
Van Eerd, J. P., & Takahashi, K. (1976) *Biochemistry 15*, 1171–1180.
Wagner, G., Pardi, A., & Wüthrich, K. (1983) *J. Am. Chem. Soc. 105*, 5948.
Zot, H. G., & Potter, J. D. (1987) *Annu. Rev. Biophys. Biophys. Chem. 16*, 535.
Zuiderweg, E. R. P. (1990) *J. Magn. Reson. 86*, 346.